

Collective dynamics in binary liquids: a molecular dynamics study of the composition dependence of the spectra of collective excitations

This article has been downloaded from IOPscience. Please scroll down to see the full text article.

2012 J. Phys.: Condens. Matter 24 505102

(<http://iopscience.iop.org/0953-8984/24/50/505102>)

View [the table of contents for this issue](#), or go to the [journal homepage](#) for more

Download details:

IP Address: 77.43.6.74

The article was downloaded on 01/11/2012 at 19:38

Please note that [terms and conditions apply](#).

# Collective dynamics in binary liquids: a molecular dynamics study of the composition dependence of the spectra of collective excitations

Taras Bryk<sup>1,2</sup> and J-F Wax<sup>3</sup>

<sup>1</sup> Institute for Condensed Matter Physics, National Academy of Sciences of Ukraine, 1 Svientsitskii Street, UA-79011 Lviv, Ukraine

<sup>2</sup> Institute of Applied Mathematics and Fundamental Sciences, National Polytechnic University of Lviv, UA-79013 Lviv, Ukraine

<sup>3</sup> Université de Lorraine, LCP-A2MC, EA4632, 1, boulevard Arago 57078 Metz Cedex 3, France

E-mail: [bryk@icmp.lviv.ua](mailto:bryk@icmp.lviv.ua)

Received 14 August 2012, in final form 15 October 2012

Published 1 November 2012

Online at [stacks.iop.org/JPhysCM/24/505102](http://stacks.iop.org/JPhysCM/24/505102)

## Abstract

The spectra of longitudinal and transverse collective excitations in liquid binary metallic  $\text{Na}_c\text{K}_{1-c}$  alloys are studied for pure components and four different concentrations.

A theoretical generalized collective modes approach is used to analyze the concentration dependence of the dispersion of acoustic and optic branches in a wide region of wavenumbers.

The dispersion of longitudinal collective excitations in binary alloys is estimated from the eight-variable thermo-viscoelastic dynamic model with full account of thermal fluctuations.

It is found that the longitudinal and transverse branches show different dependences on concentration in the short-wavelength region. The issue of ‘positive dispersion’ of acoustic excitations in liquid binary alloys on the boundary of the hydrodynamic regime is discussed.

It is shown that the coupling between longitudinal acoustic and optic modes is responsible for an increase of the ‘positive dispersion’ close to equimolar composition.

(Some figures may appear in colour only in the online journal)

## 1. Introduction

Experimental and simulation studies of the dynamic structure factors in liquid metals reveal interesting behavior of the collective excitations and fascinating features of their dispersion, that changes from a linear hydrodynamic law to a high-frequency dispersion and with further increase of wavenumbers to a roton-like minimum in the short-wavelength region [1–3]. The collective dynamics in binary metallic liquid alloys is of great interest for theoretical, experimental and simulation groups, especially since the reports on ‘fast sound’ observation in molecular dynamics simulations of  $\text{Li}_4\text{Pb}$  [4] and the later inelastic neutron scattering experiments on molten  $\text{Li}_4\text{Pb}$  and  $\text{Li}_4\text{Tl}$  [5]. The existence of two collective excitations branches in mixtures

with high component–mass ratio has been actively studied theoretically, first within the memory-function approach [6, 7], and later on using the more advanced method of generalized collective modes (GCM) [8, 9]. The GCM approach permitted the analytical conditions for the existence of transverse [8] and longitudinal [9] optic-like excitations in non-Coulombic liquid mixtures to be obtained. It also analytically explained the non-vanishing contributions from optic modes to the charge density autocorrelation functions in molten salts in the long-wavelength limit [10]. Namely, the GCM approach made it possible to explain the ‘fast sound’-like behavior of the frequency of the side peak of the dynamic structure factors as a crossover in contributions coming from the acoustic and non-hydrodynamic optic branches of collective excitations. The crossover takes place

by approaching the boundary of the hydrodynamic regime from higher wavenumbers: since the contribution from the high-frequency branch is decaying  $\propto k^2$ , whereas the contribution from acoustic modes tends to a constant in the  $k \rightarrow 0$  limit, one observes in the shape of the partial dynamic factor of the light component a ‘fast sound’-like behavior of the side peak. This was demonstrated by the GCM analysis of MD simulations performed for  $\text{Li}_4\text{Pb}$  [11] and  $\text{Li}_4\text{Tl}$  [12].

An attempt to study more generally the dependence of the dispersion branches of both collective excitations on the component mass ratio was presented in [11]; in particular, this was studied analytically in the long-wavelength limit. On the other hand, on the basis of a ‘toy model’, a concept of ‘bare’ propagating modes was introduced in [13] in order to study analytically the dispersion of purely imaginary eigenvalues over the whole wavenumber range. The ‘bare’ modes mean purely imaginary eigenvalues, i.e. there is no damping for these modes. The coupling of ‘bare’ propagating and relaxing modes causes the damping of collective excitations. Therefore, in the zero approximation one can consider ‘bare’ propagating modes which do not interact with relaxation processes [13, 14]. This simplification permits the mass ratio and concentration dependence of the dispersion of ‘bare’ collective modes in a model binary liquid to be studied analytically. Namely, for the case of ‘bare’ modes a perturbation approach for dispersion of collective excitations was suggested in [14].

Another interesting issue in the collective dynamics of liquids is the so-called ‘positive dispersion’ of collective excitations [1, 15], that emerges at the boundary of the hydrodynamic regime in dense liquids and consists of an increase of the apparent speed of sound from its macroscopic hydrodynamic value to some high-frequency value due to coupling of collective excitations with structural relaxation. However, the existing theory of ‘positive dispersion’ based on the mode coupling approach [16, 17] was unable to explain recent inelastic x-ray scattering experiments on the pressure dependence of the ‘positive dispersion’ in supercritical argon [18]. Interestingly, the ‘positive dispersion’ in supercritical fluids was suggested to be a dynamic quantity that enables a discrimination between the ‘gas-like’ and ‘liquid-like’ fluids even beyond the critical point [18, 19]. Recently, the GCM approach applied to the problem of the pressure (density) dependence of the ‘positive dispersion’ in pure fluids [20] explained correctly the features of sound dispersion in the long-wavelength region and derived a condition of vanishing ‘positive dispersion’ in the gas-like region. Very recently, an IXS experimental study conducted for a number of liquids [21, 22] successfully tested the predictions of the GCM theory on ‘positive dispersion’. The GCM predictions on ‘positive dispersion’ for pure liquids were even used for the analysis of sound dispersion in complex liquids [21, 22], that definitely is not completely consistent. To date, the theory of ‘positive dispersion’ for the case of many-component liquids has still not been elaborated, because even if a simple viscoelastic approximation is adopted for the case of binary liquids, a six-variable GCM model would have to be analytically solved in the long-wavelength

limit, which is too complicated. Simpler models like [13] point out that there should be an additional contribution to the ‘positive dispersion’ originating from the coupling between acoustic and optic modes. Therefore, an interesting issue would be to determine how such a contribution would change with concentration even in the simplest binary alloys.

To date, however, there has been no detailed study of the concentration dependence of the spectra of longitudinal and transverse collective excitations in realistic liquid mixtures or metallic binary alloys. The issue of ‘positive dispersion’ of acoustic excitations in binary liquids and its possible concentration dependence has not even been considered. Recently, we reported a GCM study of the relaxation processes in liquid metallic  $\text{Na}_c\text{K}_{1-c}$  alloys [23] in order to explain the large values of the Landau–Placzek ratio observed in simulations of these alloys. They were also studied for the dependence of the structural and diffusion properties on the concentration [24], as well as for the experimental IXS dynamic structure factor, but only at the  $\text{Na}_{57}\text{K}_{43}$  composition [25]. The potentials for these alloys are well elaborated and yield realistic results for the structural and single-particle dynamic properties. Hence, metallic  $\text{Na}_c\text{K}_{1-c}$  liquid alloys are well suited for a GCM study of collective excitations. Here, we aim to study the concentration dependence of the dispersion of longitudinal and transverse collective excitations in realistic liquid metallic  $\text{Na}_c\text{K}_{1-c}$  alloys with particular focus on the ‘positive dispersion’ of acoustic modes.

This paper is organized as follows. In section 2 we present the details of MD simulations and spectra calculations. Results on the dispersion of longitudinal and transverse collective excitations in  $\text{Na}_c\text{K}_{1-c}$  liquid alloys are given in section 3. Finally, section 4 summarizes the conclusions of this study.

## 2. Molecular dynamics simulations and the methodology of dispersion calculations

We performed classical MD simulations for the pure liquid metals Na and K and four  $\text{Na}_c\text{K}_{1-c}$  alloys with  $c = 0.2, 0.4, 0.6$  and  $0.8$  at a temperature of 373 K, a little above the melting point of Na. The effective interactions were obtained from Fiolhais’ pseudopotential [26] and the Ichimaru–Utsumi local field correction [27] (see [24] for detailed formulas and a test of the reliability of this force description). The cut-off radius was chosen at a node of the force located at about 20 Å. All the simulations were performed in the *NVT* ensemble with 4000 particles in a cubic box subject to periodic boundary conditions. Calculation of the time evolution of all relevant dynamic variables required by GCM studies is highly time consuming from MD simulations. Therefore, the earliest GCM studies of liquids [8, 28, 29] were performed with much smaller numbers of particles. Recent simulations of metallic liquid alloys with 4000 particles and their GCM analysis [12, 23] gave evidence that all the features of collective dynamics are well reproduced with systems of that size. However, liquid systems close to their melting points have hydrodynamic regions (regions of wavenumbers where the hydrodynamic

asymptotes of collective modes are observed) much narrower than high-temperature liquids far above their melting point. Thus, the size of the MD box in actual simulations of Na–K alloys (between  $L = 54.799 \text{ \AA}$  for pure Na and  $L = 68.156 \text{ \AA}$  for pure K) may not be sufficient to study the hydrodynamic regime in high detail, but this is out of the scope of our study and we will mainly focus on collective excitations near the boundary of the hydrodynamic regime.

The time step in the simulations was 10 fs and the production runs were of 300 000 steps. Each sixth configuration has been considered to sample relevant dynamic variables from which the correlation functions and generalized hydrodynamic matrix elements have been obtained. The wavevectors  $\mathbf{k}$  were sampled for our case of a cubic MD box in a standard way as

$$\begin{aligned} k_x &= 2\pi m_x/L, & k_y &= 2\pi m_y/L, \\ k_z &= 2\pi m_z/L, & m_x, m_y, m_z &= 0, \pm 1, \pm 2 \dots, \end{aligned}$$

and additional averages of static and time-correlation functions over all possible directions of wavevectors with the same module were performed. Thus,  $k$ -dependent quantities have been evaluated for 20  $k$ -values, with the smallest one ranging from  $0.09 \text{ \AA}^{-1}$  for pure K to  $0.11 \text{ \AA}^{-1}$  for pure Na.

To obtain the collective excitations spectra, we first computed the partial particle densities,  $n_\alpha(k, t)$ , the partial densities of the longitudinal/transverse mass current,  $J_\alpha^{L/T}(k, t)$ , and the energy density,  $\varepsilon(k, t)$ , via the following microscopic expressions:

$$\begin{aligned} n_\alpha(k, t) &= \frac{1}{\sqrt{N_\alpha}} \sum_{j=1}^{N_\alpha} e^{-i\mathbf{k}\mathbf{r}_j}, \\ J_\alpha^L(k, t) &= \frac{m_\alpha}{\sqrt{N_\alpha}} \sum_{j=1}^{N_\alpha} \frac{\mathbf{k}\mathbf{v}_j}{k} e^{-i\mathbf{k}\mathbf{r}_j}, \\ J_\alpha^T(k, t) &= \frac{m_\alpha}{2\sqrt{N_\alpha}} \sum_{j=1}^{N_\alpha} \frac{[\mathbf{k}\mathbf{v}_j]}{k} e^{-i\mathbf{k}\mathbf{r}_j}, \\ \varepsilon(k, t) &= \frac{1}{\sqrt{N}} \sum_{j=1}^N \varepsilon_j e^{-i\mathbf{k}\mathbf{r}_j}. \end{aligned} \quad (1)$$

In these relations,  $N_\alpha$  and  $m_\alpha$  are the number and mass of particles of the  $\alpha$ th species,  $\mathbf{r}_j(t)$  is the position and  $\varepsilon_j(t)$  is the single-particle energy of the  $j$ th particle, and  $[\mathbf{k}\mathbf{v}_j(t)]$  is the vector product of wavevector  $\mathbf{k}$  and velocity of the  $j$ th particle. In order to reach similar sufficiently high accuracy in the description of both pure metals and alloys, the analysis of longitudinal excitations was performed within a five-variable dynamic model for pure liquids

$$\mathbf{A}^{(5)}(k, t) = \{n(k, t), J^L(k, t), \varepsilon(k, t), \dot{J}^L(k, t), \dot{\varepsilon}(k, t)\} \quad (2)$$

and within an eight-variable one

$$\mathbf{A}^{(8)}(k, t) = \{n_A(k, t), J_A^L(k, t), n_B(k, t), J_B^L(k, t), \varepsilon(k, t), J_A^T(k, t), J_B^T(k, t), \dot{\varepsilon}(k, t)\} \quad (3)$$

in the case of binary mixtures. Since the longitudinal and transverse dynamics are decoupled in the hydrodynamics of non-associating fluids the transverse collective excitations

were treated separately. Similarly to the longitudinal case, the transverse excitations in pure and binary liquids were studied in the following two- and four-variable dynamic models:

$$\mathbf{A}^{(2T)}(k, t) = \{J^T(k, t), \dot{J}^T(k, t)\} \quad (4)$$

and

$$\mathbf{A}^{(4T)}(k, t) = \{J_A^T(k, t), J_B^T(k, t), \dot{J}_A^T(k, t), \dot{J}_B^T(k, t)\}. \quad (5)$$

In these expressions, the dotted quantities refer to the corresponding time derivatives. The level of time derivatives of hydrodynamic variables in these sets was restricted to the first ones. The detailed studies of collective modes in liquids with extended sets of dynamic variables including up to the third time derivatives of hydrodynamic variables reported in [8, 11, 29] gave evidence that the second and higher orders of the time derivatives of the hydrodynamic variables are responsible for collective modes with extremely short lifetime, that marginally contribute to solely short-time dynamics. These short-time collective modes have practically no effect on the dispersion of acoustic and optic excitations.

Once one has the time evolution of dynamic variables (2)–(5) from MD simulations one can use the GCM methodology to calculate the dispersion of collective excitations. The GCM approach [28, 30] permits solution of the generalized Langevin equation for the matrix of time-correlation functions with three main assumptions: (i) the chosen set of dynamic variables represents all main dynamic processes contributing to the shape of the corresponding time-correlation functions; (ii) in contrast to mode coupling theory the coupling between collective modes is treated in a local approximation; (iii) the Markovian approximation is valid for the highest order memory functions, that is, it is correct for regular (non-supercooled) liquids.

From the time evolution of the dynamic variables, the matrix  $\mathbf{F}(k, t)$  of their time-correlation functions was computed for each  $k$ -point sampled in MD simulations and each dynamic model (2)–(5) with matrix elements

$$F_{ij}(k, t = 0) = \langle A_i^*(k, t = 0) A_j(k, t = 0) \rangle, \quad (6)$$

where the asterisk means complex conjugation. The generalized hydrodynamic matrices

$$\mathbf{T}(k) = \tilde{\mathbf{F}}(k, z = 0) \mathbf{F}^{-1}(k, t = 0),$$

where  $\tilde{\mathbf{F}}(k, z = 0)$  is the matrix of Laplace-transformed correlation functions in the Markovian approximation, were estimated from the MD data avoiding any free parameters and fitting. By making use of the equality

$$\begin{aligned} \tilde{F}_{ij}(k, z = 0) &= \int_0^\infty \langle A_i^*(k, 0) \dot{A}_j(k, t) \rangle dt \\ &\equiv \langle A_i^*(k, 0) A_j(k, 0) \rangle, \end{aligned} \quad (7)$$

and definition of the correlation times

$$\begin{aligned} \tilde{F}_{ij}(k, z = 0) &= \int_0^\infty F_{ij}(k, t) dt \\ &\equiv F_{ij}(k, t = 0) \tau_{ij}(k), \quad i, j = n_\alpha, \varepsilon, \end{aligned} \quad (8)$$

for slow hydrodynamic correlations, one can easily calculate without any fit all the matrix elements of  $\tilde{\mathbf{F}}(k, z = 0)$ . In a final step, the eigenvalues of these generalized hydrodynamic matrices  $\mathbf{T}(k)$  and associated eigenvectors were calculated. The eigenvectors permit direct fit-free calculations of the contributions  $G_{ij}^\alpha(k)$  of the estimated eigenmodes to the relevant time correlation functions

$$F_{ij}^{\text{GCM}}(k, t) = \sum_{\alpha=1}^{N_v} G_{ij}^\alpha(k) e^{-z_\alpha(k)t}, \quad (9)$$

and the corresponding dynamic structure factors via time Fourier transform of expression (9) [30, 31]. In (9),  $N_v$  denotes the number of dynamic variables in the corresponding dynamic model, i.e.  $N_v = 5$  for the thermo-viscoelastic model of longitudinal dynamics in pure liquids, or  $N_v = 8$  for the binary case. Of course, as many eigenvalues as the considered dynamic variables in the corresponding dynamic model are obtained, which can either be real,  $d_\beta(k)$ , or complex,  $z_\alpha(k) = \sigma_\alpha(k) \pm i\omega_\alpha(k)$ , quantities in the cases of relaxing and propagating modes, respectively.

### 3. GCM analysis of collective excitations in Na–K liquid alloys

In this section we will first present the concentration dependence of dispersion of ‘bare’ collective modes and will discuss the effect of the coupling between acoustic and optic modes on the ‘positive dispersion’. The dispersion of collective excitations with damping for all six simulated systems will be discussed for the longitudinal and transverse cases.

#### 3.1. Longitudinal collective modes

One of the most important quantities that is needed for analysis of the dispersion of collective excitations in liquids is the structure factor  $S(k)$ . The location of the first sharp diffraction peak (FSDP) indicates the region of the de Gennes slowing down of the density fluctuations (increase of the correlation times and slowing of the decay of density–density time–correlation functions [2]) and the corresponding roton-like minimum of the dispersion law. In figure 1, we show the composition dependence of the structure factors  $S(k)$  and—for binary systems—total structure factors  $S_H(k)$ . The well-known Bhatia–Thornton total structure factor  $S_H(k)$  can be represented as a sum of the normalized generalized  $k$ -dependent compressibility  $\theta(k)$  and an additional term connected with the so-called number-concentration ‘N-C’ dilatation  $\delta(k)$  [32],

$$S_H(k) = \theta(k) + \frac{Nk_B T \delta^2(k)}{Z(k)},$$

where the factor  $Z(k) = (\partial^2 G / \partial c^2)_{T,P,N}$  is the second derivative of the Gibbs energy with respect to the concentration. The generalized  $k$ -dependent quantities  $\theta(k)$ ,  $\delta(k)$  and  $Z(k)$  were reported for Na–K alloys in [23]. For our purpose of analysis of dispersion we note that the FSDP

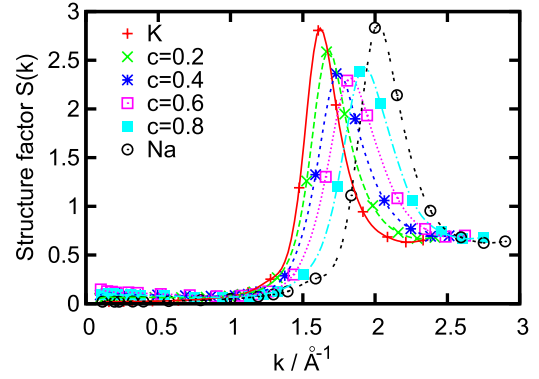


**Figure 1.** Static structure factors  $S(k)$  for pure K and Na, and  $S_H(k)$  for liquid  $\text{Na}_x\text{K}_{1-x}$  alloys at four compositions calculated via statistical averages of instantaneous total density autocorrelations. The lines represent spline interpolation of the raw data.

changes gradually with concentration from 1.6 to  $\sim 2 \text{ \AA}^{-1}$  when going from pure K to pure Na.

In order to analyze the longitudinal propagating modes it is convenient to look first at the behavior of the ‘bare’ modes [13], that can easily be obtained analytically using a reduced set of four dynamic variables,

$$\mathbf{A}^{(4)}(k, t) = \{J_\alpha^L(k, t), J_\beta^L(k, t), J_\alpha^L(k, t), J_\beta^L(k, t)\}. \quad (10)$$

The absence of dissipation processes connected with density and heat fluctuations permits one to analytically obtain two branches of non-damped excitations corresponding to the purely imaginary eigenvalues,

$$z_1^0 = \pm i\omega_1^0(k), \quad z_2^0 = \pm i\omega_2^0(k). \quad (11)$$

Both  $\omega_1^0(k)$  and  $\omega_2^0(k)$  have analytical expressions in terms of the matrix elements

$$T_{\alpha\beta}(k) = \frac{\langle J_\alpha^L J_\beta^L \rangle}{\langle J_\beta^L J_\beta^L \rangle},$$

which can be found in [13].

In the low- $k$  limit,

$$\omega_1^0(k)|_{k \rightarrow 0} = c_\infty k, \quad (12)$$

whereas

$$\omega_2^0(k)|_{k \rightarrow 0} = \omega_0, \quad (13)$$

where  $c_\infty$  corresponds to the high-frequency speed of sound and  $\omega_0$  is a constant representing the ‘bare’ frequency of the optic modes. On the other hand, in the large- $k$  limit,

$$\omega_1^0(k)|_{k \rightarrow \infty} = \left( \frac{\langle J_K^L J_K^L \rangle}{\langle J_K^L J_K^L \rangle} \right)^{1/2} = \sqrt{\frac{3k_B T}{m_K}} k \quad (14)$$

and

$$\omega_2^0(k)|_{k \rightarrow \infty} = \left( \frac{\langle J_{\text{Na}}^L J_{\text{Na}}^L \rangle}{\langle J_{\text{Na}}^L J_{\text{Na}}^L \rangle} \right)^{1/2} = \sqrt{\frac{3k_B T}{m_{\text{Na}}}} k, \quad (15)$$

giving evidence that in the Gaussian limit the low- and high-frequency branches of the collective excitations solely

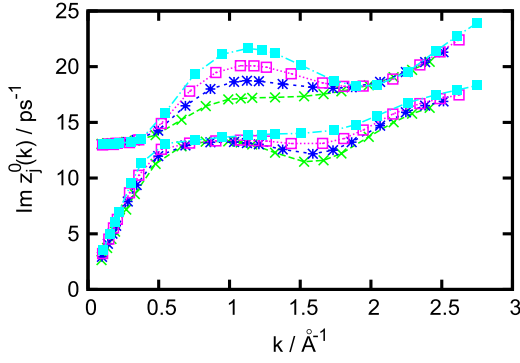


**Figure 2.** The dispersion of ‘bare’ collective modes in binary  $\text{Na}_c\text{K}_{1-c}$  liquid alloys. In the long-wavelength region the low- and high-frequency branches correspond to the acoustic and optic ‘bare’ modes, respectively. The line-connected symbols correspond to  $c = 0.2$  (crosses),  $c = 0.4$  (stars),  $c = 0.6$  (open squares) and  $c = 0.8$  (full squares).

correspond to the dynamics of the heavy (K) and light (Na) subsystems in the alloy, respectively.

In figure 2, we show the ‘bare’ collective modes calculated analytically from the correlation functions obtained in our simulations. The two eigenvalues for each binary system are shown by the same line-connected symbols, because it is impossible to discriminate beforehand between acoustic and optic branches, especially in the region where they cross. One can see that in the long-wavelength region the analytical results are recovered. Surprisingly, there is no obvious dependence of the ‘bare’ optic frequency  $\omega_0$  on the concentration. The low-frequency branch of the ‘bare’ excitations shows a linear dependence with  $k$  according to (12) in the long-wavelength region, whereas in the short-wavelength limit both branches behave according to (14) and (15). Usually, this short-wavelength asymptotic behavior can be seen beyond the roton-like minimum of the dispersion curves.

The high-frequency speed of sound,  $c_\infty(k)$ , is an important quantity for the characterization of acoustic excitations. It reflects the speed of long-wavelength collective excitations that would be based on elastic mechanisms of sound propagation (in contrast to hydrodynamic theory). The concentration dependence of the high-frequency speed of sound has been calculated from the long-wavelength limit of  $\omega_1^0(k)$ . Its changes with composition in  $\text{Na}_c\text{K}_{1-c}$  alloys are plotted in figure 3. Interestingly, it is almost a linear function of concentration, interpolating between the pure component values, which does not display any anomaly.

For comparison, in figure 3 we show the experimental values of the adiabatic speed of sound,  $c_s$ , for  $\text{Na}_c\text{K}_{1-c}$  alloys [33]. We found that these experimental data on  $c_s$  at 373 K versus Na concentration can be nicely fitted using a second order polynomial,

$$c_{\text{exp}}[\text{m s}^{-1}] = 1862.39 + 180.97c_{\text{Na}} + 464.1c_{\text{Na}}^2.$$

The two macroscopic quantities,  $c_s$  and  $c_\infty$ , are important for analysis of the ‘positive dispersion’ in liquid systems. In [20], for the case of pure liquids a correction to the hydrodynamic

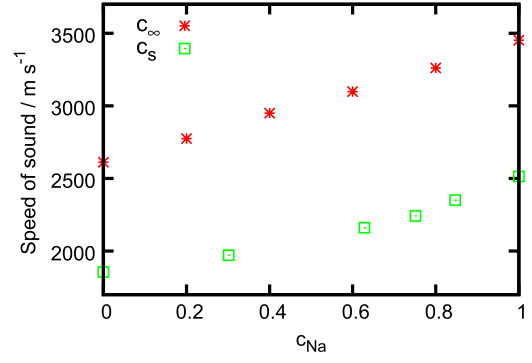


**Figure 3.** The infinite-frequency speed of sound,  $c_\infty(k)$ , as a function of concentration in liquid  $\text{Na}_c\text{K}_{1-c}$  alloys. The dependence of the experimental adiabatic speed of sound,  $c_s$ , on concentration [33] is shown by the open boxes.

dispersion law was obtained as follows:

$$\omega(k)|_{k \rightarrow 0} = c_s k + \beta k^3 + \dots, \quad (16)$$

where the factor  $\beta$  is treated as a measure of ‘positive dispersion’ [20, 34] and depends on the high-frequency and adiabatic speeds of sound, and the kinematic viscosity  $D_L$ ,

$$\beta_{\text{pure}} = \frac{c_s D_L^2}{8} \frac{5 - (c_\infty/c_s)^2}{c_\infty^2 - c_s^2} - (\gamma - 1)\Delta. \quad (17)$$

The second term in (17) with a parameter  $\Delta$  corresponds to the coupling effects between non-hydrodynamic structural and heat current relaxations. Since for  $\text{Na}_c\text{K}_{1-c}$  alloys the ratio of specific heats  $\gamma$  is close to unity (see [23]) these coupling effects can be neglected. The values of  $c_\infty$  and  $c_s$  shown in figure 3 lead to a rather smooth increase of the ‘positive dispersion’ from pure K to pure Na.

It is obvious that in binary liquids there must be an effect of the optic (LO) excitations on the ‘positive dispersion’ of the acoustic (LA) branch. As was mentioned in section 1, there does not exist to date a theory of ‘positive dispersion’ except for pure liquids. However, within the GCM approach one can make use of simplified models in order to get a clue about what kind of effect can be expected from the optic modes on ‘positive dispersion’ in binary liquid alloys. Making use of the concept of ‘bare’ modes one can show that the coupling effects between LA and LO modes depend on the  $t-x$  cross-correlations that are proportional to  $k^2$  in the long-wavelength limit (see the inset in figure 4),

$$\left. \frac{\langle J_t^L J_x^L \rangle}{\langle J_x^L J_x^L \rangle} \right|_{k \rightarrow 0} = \alpha_{tx} k^2. \quad (18)$$

Here  $\alpha_{tx}$  is the  $t-x$  cross-correlation coefficient. Then, the dispersion laws of the ‘bare’ branches can easily be obtained in the long-wavelength limit as follows:

$$\begin{aligned} \omega_1^0(k)|_{k \rightarrow 0} &\approx c_\infty k - \frac{x_1 x_2 \alpha_{tx}^2}{2c_\infty \omega_0^2} k^3, \\ \omega_2^0(k)|_{k \rightarrow 0} &\approx \omega_0 + \frac{x_1 x_2 \alpha_{tx}^2}{2c_\infty \omega_0^2} k^3. \end{aligned} \quad (19)$$

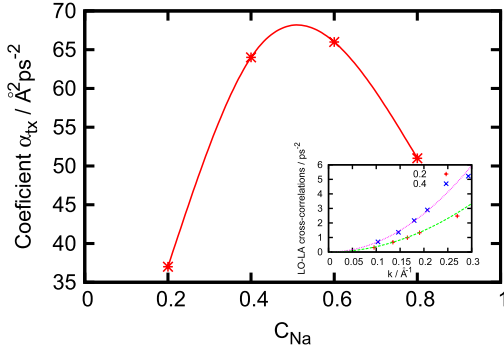


**Figure 4.** The dependence of the coupling constant between the longitudinal acoustic and optic modes on the concentration. The inset shows the cross-correlation static averages,  $\frac{\langle j_x^L j_x^L \rangle}{\langle J_x^L J_x^L \rangle}(k)$ , calculated from MD data for concentrations  $c = 0.2$  (plus symbols) and  $c = 0.4$  (crosses) and their correspondence to the correct quadratic wavenumber dependence of  $t$ - $x$  cross-correlations (18) in the long-wavelength region.

These expressions give evidence that the low- and high-frequency branches shift in opposite directions due to the coupling between them. There should be a negative contribution from the LA–LO coupling to the dispersion of the low-frequency branch and a positive contribution to the dispersion of the high-frequency branch in binary liquids. In figure 4, we show the concentration dependence of the coupling constant  $\alpha_{tx}$  for the four concentrations of  $\text{Na}_c\text{K}_{1-c}$  alloys. It follows that the largest contribution to the ‘positive’/‘negative’ dispersions of the high- and low-frequency branches should be expected for the equimolar composition. Since the optic and acoustic branches of ‘bare’ excitations cross at wavenumbers  $\sim 0.5 \text{ \AA}^{-1}$ , one can expect that the high-frequency branch,  $\omega_2^0(k)$ , for higher wavenumbers is a continuation of the acoustic dispersion, showing an additional contribution to ‘positive dispersion’ due to coupling with optic modes (19).

The dispersion curves of the propagating acoustic- and optic-like collective excitations, calculated with full account of their coupling with relaxation processes, are presented in figure 5. In the case of pure components we obviously only show the acoustic branch, although another pair of complex-conjugated eigenvalues corresponding to non-hydrodynamic heat waves,  $z_h(k)$ , was obtained for larger wavenumbers. The purely real eigenvalues that correspond to wavenumber dependent relaxation processes were discussed in detail in [23]. Here, we will only focus on the dispersion of the acoustic and optic branches (for binary alloys). For clarity, we do not show the dispersion of non-hydrodynamic heat waves,  $z_h(k)$ . They only marginally contribute to the dynamic structure factors of interest.

A noticeable fact in figure 5 is that the damping due to coupling with relaxation processes only slightly shifts the frequencies of the propagating modes down in comparison with the dispersion of ‘bare’ modes. This nice reproduction of the dispersion of collective modes in liquid alloys by simplified models, that permit analytical solutions, makes them worthwhile. The results for both pure components, also

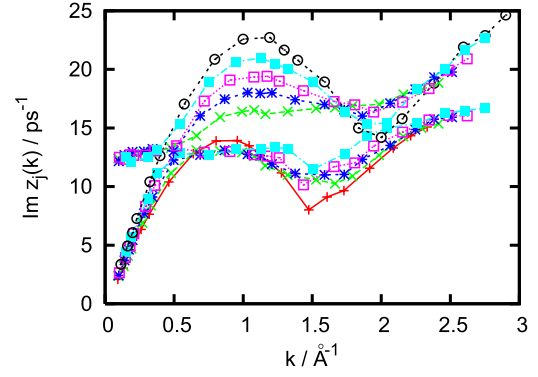


**Figure 5.** The dispersion of collective excitations in  $\text{Na}_c\text{K}_{1-c}$  liquid alloys obtained on the basis of an eight-variable dynamic model  $\mathbf{A}^{(8)}$  for binary case and a corresponding five-variable dynamic model  $\mathbf{A}^{(5)}$  for pure components. The line-connected symbols correspond to pure K (plus signs),  $c = 0.2$  (crosses),  $c = 0.4$  (stars),  $c = 0.6$  (open squares),  $c = 0.8$  (full squares) and pure Na (open circles).

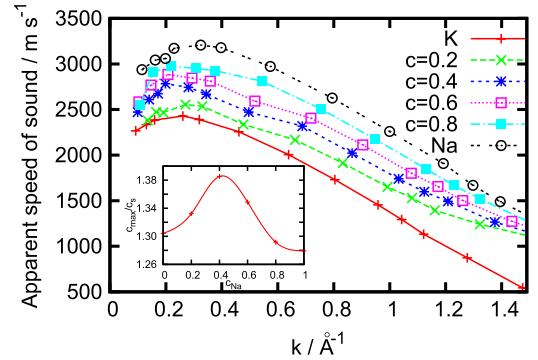


**Figure 6.** The apparent speed of sound as a function of wavenumber for liquid  $\text{Na}_c\text{K}_{1-c}$  alloys. The inset shows the ratio of the maximum of the apparent speed,  $c_{\text{max}}$ , for each concentration to the experimental adiabatic speed of sound,  $c_s$ . This ratio was defined in [18] as a measure of the ‘positive dispersion’ observed in IXS-experiment-derived dispersion curves. The concentration dependence of the ratio gives evidence that the ‘positive dispersion’ in liquid binary Na–K alloys increases for close to equimolar compositions.

plotted in figure 6, help to highlight the features of the low- and high-frequency dispersion branches for the binary liquid alloys. In the long-wavelength region, the low- and high-frequency excitations are clearly identified as acoustic and optic modes, respectively. Within the accuracy of the GCM calculations, all the longitudinal optic branches tend to a frequency  $\sim 12.3 \text{ ps}^{-1}$ . The acoustic branches for binary  $\text{Na}_c\text{K}_{1-c}$  alloys are all located between the curves of pure K (lowest branch) and pure Na (highest one). Their slope increases gradually with increasing concentration of the light component (Na).

With increasing wavenumber, the optic branches cross the corresponding acoustic ones at  $k \approx 0.5 \text{ \AA}^{-1}$ . As a consequence, for higher  $k$ -values, it is no longer possible to ascribe branches to either acoustic or optic excitations. For  $k > 1 \text{ \AA}^{-1}$ , the low- and high-frequency branches instead correspond to the partial dynamics of the heavy- and light components in the surrounding medium, respectively.

In the case of pure components, the dispersion curves have a minimum at about the location of the FSDP of  $S(k)$  (at  $k \approx 1.6 \text{ \AA}^{-1}$  in liquid K and  $k \approx 2 \text{ \AA}^{-1}$  in liquid Na). These wavenumber regions correspond to the appearance of the de Gennes slowing down of density fluctuations, and an interesting sequence of dispersion curves versus concentration is observed here for the case of binary alloys. Only the low-frequency branches contain a minimum at  $k \approx 1.6 \text{ \AA}^{-1}$ ; this value increases with increasing concentration of the light component, Na. At  $k \approx 2 \text{ \AA}^{-1}$ , only the high-frequency branches of the binary alloys have a shallow minimum. This time, interestingly, the minimum value increases with increasing concentration of the heavy component, K. Perhaps, in the region of ‘partial’ dynamics, there exists a mechanism of different damping of the longitudinal excitations corresponding to the kind of particles predominant in the surrounding medium. This composition dependence of the excitation frequencies in the region of de Gennes slowing down will be studied analytically elsewhere.

Outside the hydrodynamic regime, the acoustic excitations interact with the non-hydrodynamic structural relaxation and optic modes. The slope change of the dispersion curve outside the hydrodynamic regime can be highlighted by considering the apparent speed of sound, i.e. the apparent frequency  $\omega_s(k)$  of acoustic excitations divided by wavenumber [1]. In figure 6, we show the evolution of the apparent speed of sound with composition. The inset in figure 6 illustrates how the ratio of the maximum of the apparent speed to the adiabatic speed of sound, ascribed in [18] to ‘positive dispersion’, changes with composition for  $\text{Na}_c\text{K}_{1-c}$  alloys. It is seen that the positive dispersion is rather strong, especially close to the equimolar composition, which implies a strong effect of the LA–LO coupling on the ‘positive dispersion’, as follows from figure 4. This finding should be compared with the analytical theory of ‘positive dispersion’ in binary liquids to be developed within the GCM approach.

### 3.2. Transverse dynamics

Transverse propagating modes in pure and binary liquids are all of the non-hydrodynamic kind since they cannot survive on a macroscopic length scale. Indeed, the only conserved quantity in transverse dynamics is the transverse component of the total mass current; hence, the only hydrodynamic transverse mode existing in fluids is the relaxation process connected with the shear viscosity of the system, which cannot propagate. Therefore, transverse sound excitations cannot propagate with long wavelength, and the dispersion curve of non-hydrodynamic shear waves must start at a non-zero wavenumber,  $k_s$ . In figure 7, the branch of the shear waves reaches zero frequency at the smallest available wavenumbers,  $k_{\min}$ . Accordingly, this implies that  $k_s \simeq k_{\min}$  at each composition and that hydrodynamic shear waves are absent from the spectrum, even if the corresponding  $k$ -range is out of reach of our simulations.

In the long-wavelength region, there is a flat branch of transverse optic modes at a frequency of  $\sim 12.3 \text{ ps}^{-1}$ .

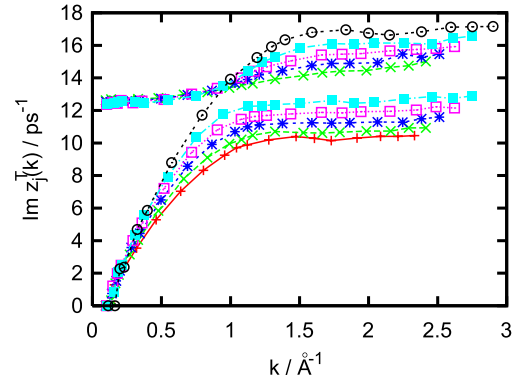


**Figure 7.** The dispersion of generalized transverse excitations in the pure components and four compositions of the Na–K alloy. The symbols are defined as before.

Similarly to longitudinal modes, the location of this long-wavelength TO branch almost does not change with composition.

Comparing the shear-waves branches of the pure components with those of the binary alloys, it can be found that both branches of all the binary alloys are located right between the branches of pure K (lowest frequency branch) and pure Na (highest frequency branch), whatever the composition, provided that  $k > 1 \text{ \AA}^{-1}$ . This is further evidence that for  $k > 1 \text{ \AA}^{-1}$  the low/high-frequency branch in binary alloys is defined by the partial dynamics of the heavy/light component in the surrounding medium. The effect of the surrounding medium is reflected in the sequence of branches versus composition: both transverse frequencies increase with the concentration of the lighter component, namely Na. For longitudinal branches in the FSDP region of pure Na, we have found a completely opposite tendency of the frequency change with composition for the high-frequency branch (see figure 5). This observation is in agreement with a memory-function study on K–Cs liquid alloys [6].

## 4. Conclusion

We have studied the composition dependence of the collective excitations for four concentrations of the binary liquid alloys  $\text{Na}_c\text{K}_{1-c}$  and the pure liquid metals K and Na. The approach of generalized collective modes was applied for calculations of the dispersion of the acoustic and optic branches.

The main conclusions of this study can be formulated as follows.

- (i) We have shown that the coupling between the acoustic and optic modes causes an increase of the ‘positive dispersion’, that can be quantitatively explained within the simplified model of ‘bare’ excitations. The prediction of this theoretical approach for the increase of ‘positive dispersion’ for compositions close to the equimolar one was supported by direct calculation of the ratio of the apparent speed of sound to the adiabatic one. These findings point out the need in analytical theory for the ‘positive dispersion’ for binary liquids, that perhaps can



be derived using the perturbation GCM theory proposed in [14].

- (ii) In the region of ‘partial’ dynamics, we have found that the dispersion of the transverse collective excitations of binary alloys is located right between the frequencies of the transverse collective modes of the pure components. Both transverse branches for binary systems showed a gradual frequency increase with the concentration of the light component.
- (iii) In contrast with the evolution with composition of the transverse branches, we have found a completely different behavior for the longitudinal excitations close to the locations of the first sharp diffraction peaks of  $S(k)$  of pure Na. In the region of the FSDP of pure K, the low-frequency branches increase with the concentration of Na, as do the transverse branches. However, in the region of the FSDP of pure Na, the high-frequency branches decrease with the concentration of Na. This implies a mechanism of stronger damping for longitudinal excitations in the region of ‘partial’ dynamics having the surrounding medium mostly of the same kind of particles.

## Acknowledgments

The simulations were performed using the SIMUL package, originally developed at the Institute for Theoretical Physics, Technische Universität Wien, and its extended custom version designed for GCM calculations. This study was partially supported by the NASU Program ‘Fundamental properties of matter in a wide range of spatial and time scales’ and Grid-project No. 0112U003269.

## References

- [1] Scopigno T, Ruocco G and Sette F 2005 *Rev. Mod. Phys.* **77** 881
- [2] Hansen J-P and McDonald I R 1986 *Theory of Simple Liquids* (London: Academic)
- [3] Boon J-P and Yip S 1980 *Molecular Hydrodynamics* (New York: McGraw-Hill)
- [4] Bosse J, Jacucci G, Ronchetti M and Schirmacher W 1986 *Phys. Rev. Lett.* **57** 3277
- [5] de Jong P H K, Verkerk P, de Vroeghe C F, de Graaf L A, Howells W S and Bennington S M 1994 *J. Phys.: Condens. Matter* **6** L681
- [6] Chushak Ya, Bryk T, Baumketner A, Kahl G and Hafner J 1996 *Phys. Chem. Liq.* **32** 87
- [7] Anento N, Gonzalez L E, Gonzalez D J, Chushak Ya and Baumketner A 2004 *Phys. Rev. E* **70** 041201
- [8] Bryk T and Mryglod I 2000 *J. Phys.: Condens. Matter* **12** 6063
- [9] Bryk T and Mryglod I 2002 *J. Phys.: Condens. Matter* **14** L445
- [10] Bryk T and Mryglod I 2004 *J. Phys.: Condens. Matter* **16** L463
- [11] Bryk T and Mryglod I 2005 *J. Phys.: Condens. Matter* **17** 413
- [12] Bryk T and Wax J-F 2009 *Phys. Rev. B* **80** 184206
- [13] Bryk T and Mryglod I 2007 *Low Temp. Phys.* **33** 790
- [14] Bryk T and Mryglod I 2008 *Condens. Matter Phys.* **11** 139
- [15] Gorelli F A, Santoro M, Scopigno T, Krisch M and Ruocco G 2006 *Phys. Rev. Lett.* **97** 245702
- [16] Ernst M H and Dorfman J R 1975 *J. Stat. Phys.* **12** 311
- [17] de Schepper I M, Verkerk P, van Well A A and de Graaf L A 1984 *Phys. Lett. A* **104** 29
- [18] Simeoni G, Bryk T, Gorelli F A, Krisch M, Ruocco G, Santoro M and Scopigno T 2010 *Nature Phys.* **6** 503
- [19] McMillan P F and Stanley H E 2010 *Nature Phys.* **6** 479
- [20] Bryk T, Mryglod I, Scopigno T, Ruocco G, Gorelli F and Santoro M 2010 *J. Chem. Phys.* **133** 024502
- [21] Bencivenga F and Cunsolo A 2012 *J. Chem. Phys.* **136** 114508
- [22] Cunsolo A 2012 *J. Phys.: Condens. Matter* **24** 375104
- [23] Bryk T and Wax J-F 2011 *J. Chem. Phys.* **135** 024502
- [24] Wax J-F 2008 *Physica B* **403** 4241
- [25] Cazzato S, Scopigno T, Bryk T, Mryglod I and Ruocco G 2008 *Phys. Rev. B* **77** 094204
- [26] Fiolhais C, Perdew J P, Armster S Q, MacLaren J M and Brajczewska M 1995 *Phys. Rev. B* **51** 14001
- [27] Ichimaru S and Utsumi K 1981 *Phys. Rev. B* **24** 7385
- [28] Bryk T, Mryglod I and Kahl G 1997 *Phys. Rev. E* **56** 032202
- [29] Bryk T and Mryglod I 2001 *Phys. Rev. E* **63** 051202
- [30] Mryglod I M, Omelyan I P and Tokarchuk M V 1995 *Mol. Phys.* **84** 235
- [31] Bryk T and Mryglod I 2001 *Phys. Rev. E* **64** 032202
- [32] Bhatia A B, Thornton D E and March N H 1974 *Phys. Chem. Liq.* **4** 97
- [33] Amaral J E and Letcher S V 1974 *J. Chem. Phys.* **61** 92
- [34] Bryk T and Ruocco G 2011 *Mol. Phys.* **109** 2929